The Hippo pathway terminal effector TAZ/WWTR1 mediates oxaliplatin sensitivity in colon cancer cells

Věra Slaninová [1#], Lisa Heron-Milhavet[1#], Mathilde Robin[1,2,3], Laura Jeanson[1], Diala Kantar[1], Diego Tosi[1,3], Laurent Bréhélin[2], Céline Gongora[1*], and Alexandre Djiane[1*]

[1] IRCM, Univ Montpellier, Inserm, ICM, Montpellier, France

[2] LIRMM, Univ Montpellier, Inserm, CNRS, Montpellier, France

[3] Fondazione Gianni Bonadonna, Milan, Italy

*Authors for correspondence: IRCM, Inserm U1194
208, rue des Apothicaires
34298 Montpellier, Cedex, France
tel: +33 (0) 411 283 157
email: alexandre.djiane@inserm.fr
celine.gongora@inserm.fr

# contributed equally

KEY WORDS:

Oxaliplatin, colon cancer, Hippo signaling, TAZ, P53

SUMMARY

YAP and TAZ, the Hippo pathway terminal transcriptional activators, are frequently upregulated in cancers. In tumor cells, they have been mainly associated with increased tumorigenesis controlling different aspects from cell cycle regulation, stemness, or resistance to chemotherapies. In fewer cases, they have also been shown to oppose cancer progression, including by promoting cell death through the action of the P73/YAP transcriptional complex, in particular after chemotherapeutic drug exposure. Using several colorectal cancer cell lines, we show here that oxaliplatin treatment led to a dramatic core Hippo pathway down-regulation and nuclear accumulation of TAZ. We further show that TAZ was required for the increased sensitivity of HCT116 cells to oxaliplatin, an effect that appeared independent of P73, but which required the nuclear relocalization of TAZ. Accordingly, Verteporfin and CA3, two drugs affecting the activity of YAP and TAZ, showed an antagonistic with oxaliplatin in co-treatments. Our results support thus an early action of TAZ to sensitize cells to oxaliplatin, consistent with a model in which nuclear TAZ in the context of DNA damage and P53 activity pushes cells towards apoptosis.

INTRODUCTION

Colorectal cancer (CRC) is the third leading cause of cancer-related death worldwide (Rawla et al., 2019). 30% of patients present synchronous metastases and 50-60% will develop metastases that will require chemotherapy. The current management of advanced or metastatic CRC is based on fluoropyrimidine (5-FU), oxaliplatin and irinotecan as single agents or more often in combination (e.g. FOLFOX, FOLFIRI, or FOLFIRINOX; Xie et al., 2020). Chemotherapy is combined with targeted therapy including monoclonal antibodies against EGFR (e.g. cetuximab and panitumumab) or VEGF (bevacizumab), tyrosine kinase inhibitors (e.g. regorafenib), and immune checkpoint blockade agents for patients with MSI-High tumors (e.g. pembrolizumab; Xie et al., 2020).

Oxaliplatin is a third-generation platinum antitumor compound with a 1,2-diaminocyclohexane (DACH) ligand (Chaney, 1995; Raymond et al., 1998). It induces mainly intra-strand crosslinks, but also inter-strand crosslinks and DNA-protein crosslinks that stop DNA replication and transcription, leading to apoptotic cell death (Perego and Robert, 2016; Woynarowski et al., 2000, 1998). Oxaliplatin exerts its anti-tumor effect also by inducing immunogenic cell death (Tesniere et al., 2010). Resistance to oxaliplatin can be either intrinsic (primary resistance) or acquired (secondary resistance), and is usually tackled by combining drugs to expose tumoral cells weaknesses or inhibit alternative survival pathways (Vasan et al., 2019). Despite intense research efforts in this field, more information on the molecular mechanisms underlying oxaliplatin mechanism of action are needed to develop new treatment strategies and improve the therapeutic response rate.

The Hippo signaling pathway represents an evolutionarily highly conserved growth control pathway. First discovered through genetic screens in *Drosophila*, it consists of a central cascade of core kinases: MST1/2 and LATS1/2 (homologues of *Drosophila* Hippo and Warts; Heng et al., 2021; Pocaterra et al., 2020; Zheng and Pan, 2019). When activated, LATS1/2 phosphorylate YAP and WWTR1/TAZ (homologues of *Drosophila* Yki), two partly redundant transcriptional co-activators which represent the terminal effector of the Hippo pathway (Reggiani et al., 2021). Phosphorylated YAP and TAZ are retained in the cytoplasm through binding to 14-3-3 proteins, and sent for proteasomal degradation. When the Hippo pathway is not activated, hypo-phosphorylated YAP/TAZ enter the nucleus and bind to specific transcription factors (TFs) to turn on the transcription of target genes. The best characterized TF partners for YAP and TAZ are the TEADs (TEAD1-4, homologues of *Drosophila* Scalloped; Heng et al., 2021; Pocaterra et al., 2020; Zheng and Pan, 2019). While depending

77 on cell type, the classic target genes include genes involved in proliferation, resistance to
78 apoptosis, cytoskeletal remodeling, or stemness (Rosenbluh et al., 2012; Tapon et al., 2002;
79 Totaro et al., 2018). But YAP/TAZ nucleo-cytoplasmic localization (and activity) is also
80 controlled by mechanical cues relayed by the actin cytoskeleton, or by cytoplasmic trapping
81 proteins such as AMOTs (Heng et al., 2021; Pocaterra et al., 2020; Zheng and Pan, 2019).
82 Importantly, the nuclear retention of YAP and TAZ is favored by tyrosine phosphorylation by
83 different kinases, and in particular SRC and YES (Byun et al., 2017; Ege et al., 2018; Li et al.,
84 2016).

85 The Hippo pathway has been primarily described as a tumor suppressive pathway in a wide
86 variety of solid tumors (Kim and Kim, 2017; Li and Guan, 2022; Nguyen and Yi, 2019;
87 Thompson, 2020; Zheng and Pan, 2019) preventing the pro-tumoral effect of YAP/TAZ.
88 However, in CRCs the role of the Hippo pathway and of YAP and TAZ appears more complex.
89 Several studies point towards a classic pro-tumoral role for YAP and TAZ. In CRC patients
90 tumor samples, high expression and nuclear localizations of YAP correlated strongly with
91 disease evolution and bad prognosis (Ling et al., 2017; Steinhardt et al., 2008), or with
92 resistance to treatments such as 5FU or cetuximab (Kim and Kim, 2017; Lee et al., 2015; Touil
93 et al., 2014). Furthermore, invalidating YAP could blunt tumorigenic behaviors both in mice
94 CRC models (Shao et al., 2014) or in the metastatic HCT116 CRC cell line (Konsavage et al.,
95 2012). However, YAP could exhibit a tumor suppressive role in CRCs. Studies in genetic
96 mouse models have shown that YAP/TAZ restricts canonical Wnt/β-Catenin signaling thus
97 preventing intestinal stem cells amplification, and could act as tumor suppressors in CRCs
98 (Azzolin et al., 2014, 2012; Barry et al., 2013). Similarly, the loss of core Hippo kinases
99 (LATS/MST) was recently shown to inhibit tumor progression in Apc mutant mouse models
100 and in patients-derived xenografts models (Cheung et al., 2020; Li et al., 2020).

101 The tumor suppressive role of YAP in CRC is further supported by its reported role in response
102 to DNA damage inducer drugs. Studies have shown that, in different cell lines including CRC
103 lines, cell death in response to cisplatin, doxorubicin, or etoposide, is mediated by P73, a
104 protein related to the tumor-suppressor P53. Following treatments, a YAP/P73 complex
105 accumulates in the nucleus, and triggers the transcription of P73 target genes involved in cell
106 death (Lapi et al., 2008; Strano et al., 2005, 2001). The direct interaction between YAP and
107 P73 is proposed to prevent P73 destabilization by the E3-Ubiquitin Ligase ITCH (Levy et al.,
108 2007; Strano et al., 2005). This pro-apoptotic role of YAP is reminiscent to a similar role of
109 Yki in *Drosophila* (a Yki/p53 complex; Di Cara et al., 2015). Importantly, this appears specific

110 to YAP, since TAZ cannot bind to P73, further suggesting that YAP and TAZ, while
111 performing redundant roles, also possess specific activities (Reggiani et al., 2021).

112 Given that oxaliplatin constitute one of the most used drugs in the treatment of CRCs, it is
113 important to evaluate its effects with respect to the Hippo pathway and to YAP/TAZ which can
114 elicit conflicting roles to oppose or promote CRC tumorigenesis. We show here that upon
115 treatment with oxaliplatin, TAZ accumulated in the nucleus of CRC cell lines. We further show
116 that TAZ was required for early sensitivity of HCT116 to oxaliplatin. Interestingly, the nuclear
117 localisation of TAZ was important, and drugs preventing this such as Dasatinib antagonized
118 the effect of oxaliplatin. These results support an early anti-tumoral role of YAP and TAZ in
119 response to oxaliplatin suggesting particular attention to sequence of treatments and drug
120 combinations should be paid when considering potential future drugging of YAP/TAZ
121 signaling in the treatment of CRCs.

122

123 **RESULTS and DISCUSSION**

124 ***Oxaliplatin treatment triggers an early cell death program***

125 Oxaliplatin is a third generation platinum compound widely used as part of the first line of
126 treatment for colon cancer patients in the FOLFOX regimen (Chaney, 1995; Raymond et al.,
127 1998; Xie et al., 2020). Inside cells, oxaliplatin binds DNA, generating adducts which
128 ultimately lead to DNA breaks and replicative stress in proliferating cells. When used on
129 proliferating cancer cells, oxaliplatin treatment resulted in concentration-dependent cell death.
130 We measured the IC50 of oxaliplatin on HCT116 colon cancer cells at 0.5µM (Supplemental
131 Figure S1A). This dose reduced the amount of cells by 50% after 4 days of treatment. This
132 dose was about 10 fold lower than the oxaliplatin concentration reported in the blood of treated
133 patients (between 3.7 and 7µM; Graham et al., 2000). The oxaliplatin dose used in this study
134 was thus compatible with the dose that could be ultimately found at the level of tumors in a
135 clinical setting, and did not represent an acute high concentration treatment, highlighting its
136 relevance for studying cellular responses to oxaliplatin.

137 When treated with oxaliplatin at IC50, HCT116 cells exhibited clear signs of DNA damage
138 such as accumulation of γH2AX, and 53BP1 puncta in the nuclei (Figure 1A&B). Consistently,
139 P53, which has been shown to control a specific cell death program in response to severe DNA
140 damage (for recent reviews Abuetabh et al., 2022; Panatta et al., 2021), accumulated strongly
141 24h after treatment (Figure 1C). Intriguingly, the P53 related protein P73, previously reported
142 to accumulate and to mediate cell death in response to DNA-damage inducing drugs such as
143 cisplatin, doxorubicin or etoposide, including in HCT116 cells (Lapi et al., 2008; Strano et al.,
144 2005), was destabilized upon oxaliplatin treatment. P63, the third member of the P53 protein
145 family, was not expressed in HCT116, even upon treatment (Figure 1C).

146 To better understand the cellular responses to oxaliplatin we profiled the changes in gene
147 expression after 24h of exposure at IC 50. This analysis revealed that the expression of only a
148 limited number of genes were affected (fold change >1.5, adjusted p-value < 0.05): 253 up-
149 regulated and 111 down-regulated (Figure 1D; Supplemental Table 1). Gene ontology
150 enrichment approaches using the g:profiler online tool (Supplemental Table 2; Raudvere et al.,
151 2019) highlighted that amongst the main cellular processes controlled by the upregulated genes
152 were DNA damage response (GO:0044819 mitotic G1/S transition checkpoint signaling;
153 GO:0000077 DNA damage checkpoint signaling…), apoptosis and cell death (GO:0045569
154 TRAIL binding; GO:0008219 cell death; GO:0012501 programmed cell death; GO:0006915
155 apoptotic process …), and p53 response (GO:0072331 signal transduction by p53 class

156 mediator), consistent with the known role of oxaliplatin generating adducts on the DNA.
157 Indeed, many genes up-regulated have previously been associated with p53 signaling, and
158 represent p53 canonical target genes such as CDKN1A/P21, P53I3, BAX, or TIGAR
159 (REAC:R-HSA-3700989 Transcriptional Regulation by P53; WP:WP4963 p53 transcriptional
160 gene network). While up-regulated genes controlled mainly cell death programs, the down-
161 regulated genes were involved in DNA replication (GO:0006260) and cell cycle (GO:0007049)
162 consistent with the well documented effect of DNA damage on blocking cell cycle and
163 proliferation (Abuetabh et al., 2022).
164 Amongst the genes mis-regulated were also genes related to inflammation and immune cell
165 recruitment (e.g. the upregulated genes CXCR2, EBI3/IL-27, or NLRP1, and the
166 downregulated gene IL17RB) consistent with the previously reported role of oxaliplatin during
167 immune cell death (Tesniere et al., 2010).
168 Finally, these analyses also highlighted several genes involved in cell architecture, namely
169 cytoskeleton and junctional complexes. Amongst the most striking features were changes in
170 the expression of integrin and extracellular matrix proteins engaging Integrins and Focal
171 Adhesions: collagens COL5A1 and COL12A1, as well as laminins LAMA3, LAMB3, and
172 LAMC1 and integrin ITGA3. These observations suggest that treated cells might remodel their
173 extracellular matrix, their Focal Adhesions, and the signaling pathways associated. The RNA-
174 Seq analyses revealed also many changes to the cytoskeleton, including an upregulation of
175 several keratin-based intermediate filaments (KRT15/19/32) and associated factors (KRTAP2-
176 3 and SFN). Several genes controlling the actin cytoskeleton were also affected such as the
177 branched actin regulators WDR63, CYFIP2, or WASF3, or different genes predicted to control
178 RHO activity (up: RHOD, EZR, and RAP2; down: ARHGAP18).
179
180 Taken together, these results suggest that upon oxaliplatin treatment, HCT116 cells implement
181 an early cell death program, which is likely mediated by the elevated P53 levels, and many
182 "bona-fide" P53 direct target genes involved in cell death are upregulated. Unlike other
183 treatments such as cisplatin, doxorubicin, and etoposide (Lapi et al., 2008; Strano et al., 2005),
184 oxaliplatin is unlikely to mobilize the p73 anti-tumoral response since P73 levels are decreased
185 upon oxaliplatin treatment. The difference is striking when considering closely related
186 platinum compounds such as cisplatin and oxaliplatin. This difference is unlikely due to timing
187 as we could not observe any P73 up-regulation after oxaliplatin treatment even after shorter or
188 longer exposures. Even though dose comparisons between different compounds is tricky, we
189 note that the cisplatin dose was 50 times higher than that of oxaliplatin. Alternatively, while

190 both are thought to act primarily as generators of lethal amounts of DNA breaks, their
191 difference in mobilizing either P73 (cisplatin) or P53 (oxaliplatin) might arise from different
192 alternative cellular effects independent of DNA damage.
193
194 ***Oxaliplatin treatment triggers YAP and TAZ nuclear accumulation***
195 Having established a regimen for treating HCT116 cells with oxaliplatin, and given the
196 complex reported roles of YAP/TAZ in CRCs (see Introduction), we investigated whether
197 YAP/TAZ could be affected, and thus monitored TEAD, YAP, and TAZ expressions and
198 localizations following oxaliplatin treatment.
199 After 24h (or 48h) of oxaliplatin treatment at the IC50, we did not observe any change in the
200 total levels or in the nuclear localization of TEAD4, the main TEAD paralogue in colon cells
201 (Figure 2A). However, TAZ and YAP nuclear localizations increased following oxaliplatin
202 treatment in our culture conditions: the TAZ and YAP nuclear staining increased by 60% and
203 55% respectively when compared to untreated cells (Figure 2A). TAZ nuclear accumulation
204 was also observed in two other CRC cell lines: LoVo and Caco-2 (Supplemental Figure S2).
205 TAZ nuclear accumulation was further confirmed by fractionation experiments (Figure 2C; see
206 Materials and Methods). This increase in TAZ nuclear localization was reflected by an increase
207 in total TAZ levels by western blot analysis (Figure 2B). However, YAP total levels, and more
208 importantly the levels of YAP phosphorylation on Serine 127 (S127) were unchanged (Figure
209 2B).
210 The YAP S127 phosphorylation is deposited by the LATS1/2 Hippo pathway terminal kinases
211 and mediate the cytoplasmic retention of YAP by the 14-3-3 proteins and later targeting for
212 proteasomal degradation (Heng et al., 2021; Pocaterra et al., 2020; Zheng and Pan, 2019).
213 Western-blot analyses on total protein extracts showed that several key proteins in the core
214 Hippo pathway were hypo-phosphorylated (p-MST1/2, p-MOB1) indicating a general lower
215 activity of the core Hippo pathway (Figure 2B). Total protein levels were also lower after
216 treatment, further suggesting a lower Hippo pathway activity in response to oxaliplatin,
217 consistent with the increased TAZ levels and increased nuclear TAZ localization (Figure
218 2A&C). However, given that levels of phospho-YAP and total YAP remained unchanged, how
219 the Hippo pathway down-regulation could have differing effects on YAP and TAZ remains to
220 be explored. YAP and TAZ appear only partly redundant, and YAP and TAZ specific
221 regulations have been reported (Reggiani et al., 2021). It is noteworthy that an additional
222 phospho-degron is present in TAZ, making it more sensitive to degradation than YAP. This
223 increased sensitivity might magnify TAZ level changes when the Hippo pathway is inhibited

224 by oxaliplatin (Azzolin et al., 2012). The decreased protein levels of different Hippo pathway
225 components in response to oxaliplatin were unlikely due to reduced mRNA abundance, since
226 we did not observe any change in our RNA-Seq, suggesting that it might be a consequence of
227 reduced translation and/or increased protein degradation. Indeed, previous studies have shown
228 that core Hippo pathway components can be regulated by ubiquitination such as LATS1 or
229 MOB1 (Ho et al., 2011; Lignitto et al., 2013; Salah et al., 2011). Whether oxaliplatin treatment
230 triggers a specific ubiquitin-mediated destabilization of the core Hippo pathway remains
231 however to be studied.
232
233 ***YAP is dispensable for Oxaliplatin-mediated cell death***
234 Performing pathway analyses on the mis-regulated genes highlighted a strong activation of
235 p53 signaling (Supplemental Table S2). Motif enrichment analyses suggested that the p53
236 family of transcription factors were the main controllers of the up-regulated genes. With the
237 exception of Axl, none of the "classic" YAP/TAZ target genes such as CTGF, CYR61/CCN1,
238 or BIRC2 (or genes involved in cell cycle progression, cytoskeleton regulation, or drug
239 resistance; (Pocaterra et al., 2020; Totaro et al., 2018) were up-regulated after oxaliplatin
240 treatment. We thus wondered what would be the role of YAP and TAZ in the response to
241 oxaliplatin treatment. Indeed, other anti-cancer drugs such as cisplatin have been shown to
242 promote cell death in part through the implementation of a P73/YAP-dependent cell death
243 program. Mechanistically, it has been proposed that DNA damage induced by cisplatin
244 stabilizes YAP which then binds and protects P73 from ITCH-mediated degradation (Levy et
245 al., 2007); the P73/YAP complex accumulates in the nucleus to turn on the expression of P73
246 target genes involved in cell death (Lapi et al., 2008; Strano et al., 2005, 2001). We thus
247 wondered whether the accumulation of TAZ (and the moderate accumulation of YAP) in the
248 nucleus could also participate in the cell death induced by oxaliplatin.
249 To test the requirement of YAP and TAZ, we invalidated YAP and TAZ by RNA interference.
250 The sole invalidation of YAP by shRNA led to a very modest reduction in oxaliplatin
251 sensitivity (IC50 in *shYAP* was determined at 0.62 compared to 0.52 in *shLuc* controls) (Figure
252 3A&C). It is noteworthy that, under the culture conditions used, YAP appeared dispensable for
253 HCT116 cells since the shRNA led to a knock-down efficiency >90%. These results suggest
254 that the cell death in response to oxaliplatin might not be dependent (or only marginally) on
255 the YAP/P73 complex as previously reported for other DNA-damage inducing compounds
256 (Lapi et al., 2008; Levy et al., 2007; Strano et al., 2005), but depends on alternative
257 mechanisms.

258

259 ***TAZ promotes cell death in response to oxaliplatin, independently of P73***

260 We then investigated the role of TAZ. Strikingly, while the depletion of YAP had hardly
261 any effect, the combined knock-down of both YAP (*shYAP*) and TAZ (*siTAZ*), resulted in a
262 clear increase in resistance to oxaliplatin, where the IC50 reached 0.91µM in *shYAP/siTAZ*
263 HCT116 cells compared to 0.58µM in *shLuc/siScrambled* HCT116 control cells (Figure
264 3B&C), highlighting that TAZ participates to cell death in response to oxaliplatin. The effects
265 observed were specific to the *siTAZ*, since we observed a re-sensitization of treated cells when
266 complementing them with an expression vector for a murine version of *Taz* insensitive to the
267 *siTAZ* designed against human *TAZ* (Supplemental Figure S3A&B). We then wondered
268 whether the increased sensitivity promoted by TAZ could be dependent on P73, in a similar
269 mechanism as proposed for cisplatin. However, while P53 accumulated in response to
270 oxaliplatin in HCT116, P73 levels were decreased, undermining the role of P73 in response to
271 this drug (Figure 1C). This absence of P73 stabilization, is consistent with the absence of
272 increased YAP levels after oxaliplatin treatment (Figure 2B). These results highlight that,
273 although overexpressed YAP could bind and stabilize endogenous P73 (Supplemental Figure
274 S4; Levy et al., 2007; Strano et al., 2005, 2001), oxaliplatin treatments at the clinically relevant
275 doses used, do not lead to YAP and P73 stabilization. We then confirmed that TAZ cannot bind
276 P73 (Supplemental Figure S4), ruling out that the elevated nuclear TAZ following oxaliplatin
277 could act through a transcriptional complex with P73 to enhance cell death. A recent study
278 reported a direct interaction between TAZ and P53 in MCF7 and HCT116 cells, which resulted
279 in the inhibition of P53 activity towards senescence (Miyajima et al., 2020). However, when
280 we performed co-immunoprecipitation experiments, we were unable to document any
281 interaction between over-expressed YAP or overexpressed TAZ with endogenous P53 in
282 normal or oxaliplatin treated HCT116 cells (Supplemental Figure S4). Furthermore, the
283 increased oxaliplatin resistance of cells upon *YAP/TAZ* knockdown supports strongly that TAZ
284 acts to promote cell death and thus cooperates with P53 rather than antagonizes its activity as
285 suggested before (Miyajima et al., 2020). Taken together, these results suggest that the
286 sensitivity of HCT116 cells to oxaliplatin mediated by YAP and TAZ is not mediated by the
287 direct interaction of YAP or TAZ to P53 or P73.

288

289 ***Increased resistance to oxaliplatin upon YAP/TAZ activity blockade***

290 The sh/siRNA interference results suggested that TAZ was required for sensitivity to
291 oxaliplatin. To validate independently the knock-down experiments, we used a

292 pharmacological approach with drugs targeting YAP/TAZ activity and monitored their action
293 in combination with oxaliplatin. We performed 2D matrices co-treatment analyses in which
294 cells were treated with increasing amounts of oxaliplatin and of the YAP/TAZ inhibitors
295 verteporfin or CA3 (Figure 3D and Supplemental Figure S1B &C; Liu-Chittenden et al., 2012;
296 Song et al., 2018). In both cases, the co-treatments led to a marked increase in the HCT116
297 resistance to oxaliplatin. Similar results were obtained on two other CRC cell lines: LoVo, and
298 Caco-2 (Supplemental Figure S3C&D). The mode of action of verteporfin remains unclear and
299 might involve increased retention in the cytoplasm of YAP and TAZ, or their degradation,
300 preventing them from complexing in the nucleus with their transcription factor partners (Wang
301 et al., 2016). A recent study showed that CA3 reduced the transcriptional activity mediated by
302 YAP/TAZ-TEAD (reduction in target genes expression), with only minor effects on YAP
303 protein levels (Morice et al., 2020). Even though the exact mode of action of verteporfin and
304 CA3 remain unclear, the increased resistance to oxaliplatin observed by co-treating cells with
305 YAP/TAZ pharmacological inhibitors, confirms the results obtained with the genetic knock-
306 down, and supports a model where increased TAZ activity participate in the sensitivity of CRC
307 cells to oxaliplatin.
308
309 ***Src inhibition by Dasatinib reduces HCT116 cells sensitivity to oxaliplatin***
310 The results suggest thus that preventing TAZ signaling in the early phases of oxaliplatin
311 treatment would represent a counter-productive approach, leading to reduced efficacy of
312 oxaliplatin to induce cell death. Besides the canonical Hippo signaling pathway, the nucleo-
313 cytoplasmic shuttling of YAP and TAZ is under the control of many other inputs. In particular,
314 YAP and TAZ retention in the nucleus is promoted by the action of different tyrosine kinases,
315 such as ABL or SFKs (Src Family Kinases) which phosphorylate the C-termini of YAP and
316 TAZ (Y357 or Y316 respectively; Byun et al., 2017; Ege et al., 2018; Guégan et al., 2022;
317 Kedan et al., 2018; Lamar et al., 2019; Li et al., 2016). Due to its high relevance for colon
318 cancer, we focused our analysis on SRC, frequently activated in colon carcinoma (Sirvent et
319 al., 2020). An earlier study showed that depending on the colon cancer cell line considered,
320 SRC could be activated, inhibited, or not affected following oxaliplatin treatment (Kopetz et
321 al., 2009). We could replicate that SRC was not activated after 24h of oxaliplatin treatment in
322 HCT116 cells (as measured by phosphorylation on Y416; Figure 4A). Working with HCT116,
323 we are thus in a position to test the contribution of SRC to YAP/TAZ shuttling during
324 oxaliplatin treatment without the complications arising from treatment-induced acute SRC
325 activation. Previous reports suggested that the classic SRC kinase inhibitor Dasatinib could be

326 used as a drug to prevent YAP/TAZ signaling (Rosenbluh et al., 2012). Indeed, combining
327 Dasatinib with oxaliplatin treatment, prevented the nuclear accumulation of TAZ (Figure 4B).
328 The addition of Dasatinib to oxaliplatin treated cells led to a dramatic reduction of the TAZ
329 nuclear staining when compared to oxaliplatin alone (95% reduction; see Materials and
330 Methods). It should be noted however, that Dasatinib treatment at 50nM reduced slightly the
331 elevated global TAZ levels observed in response to oxaliplatin (Figure 4A). Nevertheless, even
332 though TAZ appeared a bit more unstable in presence of Dasatinib, its nucleo-cytoplasmic ratio
333 was still profoundly affected by Dasatinib, preventing nuclear accumulation (Figure 4B).
334 We thus asked what would be the combined effect of Dasatinib treatment and oxaliplatin in
335 HCT116 cells. We thus performed 2D matrices co-treatment analyses in which cells were
336 treated with increasing amounts of oxaliplatin and of Dasatinib using drug ranges
337 encompassing their respective IC50 (0.5µM for oxaliplatin and 8µM for Dasatinib;
338 Supplemental Figure S1A&D). Strikingly combining both drugs showed clear regions of
339 antagonism, suggesting that Dasatinib treatment reduced HCT116 cells sensitivity to
340 oxaliplatin (Figure 4C). These results further support a model in which the nuclear
341 relocalization of TAZ in response to oxaliplatin treatment sensitizes cells, and caution the use
342 of Dasatinib in combination to oxaliplatin.
343
344 ***YAP/TAZ promote cell death in the early response to chemotherapeutic agents***
345 Taken together the results presented here show that oxaliplatin promotes the fast nuclear
346 relocalization of TAZ which then participates to the cells sensitivity to oxaliplatin. Given that
347 we could not find any interaction between TAZ and P53 family members, but that the nuclear
348 localization of TAZ is required for its effect, we could envision several models:
349 i) either the TAZ/TEAD transcription complex, in the context of DNA damage and P53
350 activation, promotes the transcription of specific early response genes promoting cell death;
351 ii) or the slight increase at the transcriptional level of "classic" YAP/TAZ/TEAD targets
352 involved in proliferation sensitizes cells to DNA damage and replicative stress;
353 iii) or alternatively, TAZ acts through a new complex involved in cell death, independently of
354 TEAD.
355 More studies should help to distinguish between these potential models.
356
357 YAP and TAZ, have been implicated in the resistance to various chemotherapies or targeted
358 therapies in different cancers (Kim and Kim, 2017; Nguyen and Yi, 2019; Zeng and Dong,
359 2021). It should be noted that the current study focuses on the immediate effects of oxaliplatin

360 within the first hours after exposure. Whether YAP and TAZ are later important for the
361 maintenance of the resistance acquired by the surviving clones is not addressed in this study.
362 Hints towards this later role of YAP/TAZ, are suggested by the elevated YAP levels reported
363 in many cancer cells following resistant clone selection (our own unpublished results, and (Kim
364 and Kim, 2017; Nguyen and Yi, 2019; Zeng and Dong, 2021). Functional studies impairing
365 YAP demonstrated that YAP is indeed required for the tumorigenicity of resistant cells
366 (Yoshikawa et al., 2015). Furthermore, elevated YAP and TAZ nuclear staining is frequently
367 observed in patients tumor samples, including in CRCs (Li and Guan, 2022; Ling et al., 2017;
368 Steinhardt et al., 2008; Thompson, 2020). In advanced cancers, almost all patients undergo one
369 or more rounds of treatment before surgery, if surgery is possible. It is thus unclear whether
370 the increased YAP/TAZ nuclear levels observed in tumor samples reflect primary response to
371 treatment (as suggested by the current study), or whether they represent a secondary state that
372 might have been selected in the cells resistant to treatment.
373 The current study investigates the early response to oxaliplatin, supporting an early tumor
374 suppressive role of YAP/TAZ in response to treatment, in which, in the context of detrimental
375 DNA damage, YAP/TAZ activity promotes cell death. Is this role general or is it specific to
376 CRCs and oxaliplatin? Independently of the mechanism involved (YAP/P73 complex as
377 previously reported or alternative TAZ-mediated mechanisms as shown here), different breast
378 and colon cancer cell lines mobilize YAP or TAZ to promote cell death in response to many
379 different DNA damaging agents (Basu et al., 2003; Lapi et al., 2008; Levy et al., 2007; Strano
380 et al., 2005, 2001). This anti-tumoral role appears evolutionarily conserved and in *Drosophila*
381 the YAP/TAZ homologue Yki promotes cell death in response to different stress inducing
382 agents (Di Cara et al., 2015), further suggesting that YAP/TAZ might promote cell death in
383 response to chemotherapeutic agents in other cancers beside CRCs and breast cancers. When
384 considering drugging YAP/TAZ signaling in the treatment of CRCs and other cancers, special
385 attention should thus be given to drug combinations, and importantly the sequence in which
386 they will be used.
387

388 **MATERIALS AND METHODS**

389 ***shRNA construction***

390 shRNA directed against human *YAP*, *TAZ*, or the non-relevant *Luciferase* gene were designed
391 by adding to the selected targeted sequences, overhangs corresponding to BamHI and EcoRI
392 cloning sites at the 5'end of forward and reverse strand, respectively. Resulting oligos were
393 then annealed together and cloned into the pSIREN-RetroQ vector (TaKaRa) according to the
394 manufacturer's protocol between BamHI and EcoRI cloning sites.

395 Targeted sequences:

396 *shRNA-YAP(3619):* CAATCACTGTGTTGTATAT

397 *shRNA-TAZ(1417):* CCCTTTCTAACCTGGCTGT

398 *shRNA-Luciferase:* CGTACGCGGAATACTTCGA

399

400 ***Cell culture and cell transfections***

401 Certified Human HCT 116 and LoVo colorectal cancer cell lines (RRID:CVCL_0291,
402 RRID:CVCL_0399) were obtained from LGC Standards (ATCC-CCL-247, ATCC-CCL-229).
403 Caco-2 cells (RRID:CVCL_0025) were certified independently. Cells were cultured in
404 RPMI1640 supplemented with 10% FBS at 37ºC in a humidified atmosphere with 5% CO_2.
405 Cultures were regularly checked to be mycoplasma-free. No antibiotics were used to avoid any
406 cross-reaction with the Oxaliplatin treatment.

407 HCT116 cells expressing shRNA against *YAP*, *TAZ* , or *Luciferase* (Luc; control) were
408 obtained by retroviral gene transduction of the corresponding pSIREN vectors. Retroviral
409 particles were produced in HEK293 cells and subsequently used to infect HCT116 cells.
410 Positive clones were selected with 1 µg/mL puromycin and pooled together.

411 HCT116-*shYAP/siTAZ* cells were created by transfecting 100nM of *TAZ siRNA* (Dharmacon
412 siGENOME SMARTpool #M-016083-00-0005) into HCT116-*shYAP* cells using
413 Lipofectamine 2000 (Invitrogen) according to manufacturer's protocol. As a negative control,
414 100nM of *siScrambled* (D-001206-13) was transfected into HCT116-*shLuc* cells.

415 Murine Taz was expressed by transfecting cells with pEF-TAZ-N-Flag from Michael Yaffe
416 (Addgene #19025; RRID:Addgene_19025; Kanai et al., 2000).

417

418 ***RNA-Seq***

419 HCT 116 cells were plated to reach 60 to 70% of confluence and treated with 0.5 µM
420 Oxaliplatin (IC_{50}) for 24 hours. RNA was extracted using RNeasy plus mini kit (Qiagen),

421 quantified and analyzed for its integrity number (RIN) using a Bioanalyzer (Agilent 2100 at
422 the IRMB: https://irmb-montpellier.fr/single-service/transcriptome-ngs/). RNA (1 µg) with
423 RIN between 8 and 10 were sent for RNA-Sequencing analysis to Fasteris biotechnology
424 company (http://www.fasteris.com). After library preparation, sequencing was performed on
425 the Illumina NovaSeq 6000 platform (S1 2x100 full FC). Mapping on the human genome
426 GRCh38 was performed using the protocol STAR 2.7.5b leading to 80-100 Millions reads per
427 condition. Normalization and pairwise differential expression analyses were performed using
428 the R package DESeq2 (2.13) (Anders and Huber, 2010).
429 RNA-Seq data has been deposited in NCBI's Gene Expression Omnibus under accession
430 number GSE227315.
431
432 ***Western blotting***
433 Proteins issued from transfected untreated and treated HCT 116 cells were extracted, analyzed
434 by SDS-PAGE. Dilutions and antibodies' references are listed below.
435 Flag M2 (1/2000; Sigma-Aldrich #F1804)
436 GAPDH (1/3000; Proteintech #60004)
437 Histone H3 (1/1000; Cell Signaling Technology CST #4499)
438 LATS1 (1/1000; CST #3477)
439 MOB1 (1/1000; CST #13730)
440 p-MOB1 (1/1000; CST #8699)
441 MST1 (1/1000; CST #3682)
442 p-MST1/2 (1/1000; CST #49332)
443 NF2 antibody (Proteintech #26686-1-AP)
444 P53 (1/5000; Proteintech #10442-1-AP)
445 P63 (1/250; Santa Cruz #sc25268)
446 P73 (1/1000; CST #14620)
447 p-SRC Y416(1/1000; CST #2105)
448 TAZ (1/1000; CST #4883)
449 TEAD4 (1/250; Santa Cruz #sc101184)
450 Tubulin (1/10000; Sigma-Aldrich #T6074)
451 YAP (1/1000; CST #14074)
452 p-YAP S127 (1/1000; CST #13008)
453
454 ***Immunoprecipitation and co-immunoprecipitation***

455 Protein extracts were prepared in lysis buffer (NaCl 150 mM, Tris pH 7.4 10 mM, EDTA 1
456 mM, Triton X-100 1%, NP-40 0.5%, cOmplete, EDTA-free protease inhibitors (Roche
457 #11873580001) for 30 min on ice before centrifugation. Immunoprecipitations were performed
458 overnight at 4°C on a rocking wheel using mouse EZview Red anti-Flag M2 affinity gel
459 (Sigma-Aldrich #F1804) after transfections of either p2xFlag CMV2 (empty vector), p2xFlag
460 CMV2-YAP2 (YAP1; Addgene #19045) or p2xFlag CMV2-WWTR1 (TAZ). After Flag
461 immunoprecipitation, washes in lysis buffer were performed, followed by protein elution by
462 competition with 3XFLAG peptide (150 ng/µL final concentration) during 1 hour at 4°C. The
463 different immunoprecipitates were then subjected to Western blotting for detection of protein
464 complexes.
465
466 ***Immunofluorescence***
467 Cells seeded on glass coverslips were fixed 10 min in paraformaldehyde (4 %), before being
468 permeabilized in PBS / 0.1% TritonX-100 for 10 min. After blocking in PBS / 0.5% BSA, cells
469 were incubated with primary antibodies overnight at 4C. Primary antibodies used are listed
470 below. Secondary Alexa Fluor Antibodies (1/600; Invitrogen) were used as described
471 previously (Kantar et al., 2021) for 1 hour at room temperature before mounting the coverslips
472 with Vectashield (Vector Laboratories #H-1200) and imaging on Zeiss Apotome or Leica
473 Thunder microscopes.
474 Antibodies used were rabbit anti-53BP1 (1/100; CST #4937), mouse anti-phospho-Histone
475 H2AX clone JBW301 (1/200; Millipore #05-636), anti-TAZ (1/100; CST #4883), mouse anti-
476 TEAD4 (1/50; Santa Cruz #sc101184), and rabbit anti-YAP (1/100; CST #14074).
477
478 ***Nuclear staining quantifications in HCT116 cells***
479 Quantification was performed using ImageJ. Binary mask corresponding to the cell nuclei was
480 based on DAPI staining. Two nuclei touching each other (and therefore recognized as one on
481 binary mask) were manually separated by drawing a 2-pixel line between them. All incomplete
482 nuclei on the edge of the image as well as those that were in mitosis or mechanically damaged
483 were excluded from the analysis. The total signal was calculated as "corrected total cell
484 fluorescence" (CTCF) according to the following formula:
485 *CTCF = Integrated Density – (Area of selected cell * Mean fluorescence of the background)*
486 Background fluorescence was measured on three different spots (roughly the size of cell
487 nucleus) outside of the cell. In case of 53BP1 and g-H2AX staining, the whole area covered by
488 the nuclear mask was quantified as one. For YAP and TAZ nuclear staining, each cell was

489 quantified separately using particle analysis tool. Cytoplasmic levels of YAP and TAZ were
490 not quantified due to the small size of the cytoplasm in HCT116 cells.
491
492 ***IC50 calculation and cytotoxicity***
493 Cell growth inhibition and cell viability after incubation with Oxaliplatin (Sigma Aldrich
494 #O9512), Verteporfin (Sigma Aldrich #SML0534), CA3 (CIL56, Selleckchem, #S8661) or
495 Dasatinib (Selleckchem #S1021) were assessed using the sulforhodamine B (SRB) assay.
496 Exponentially growing cells (750 cells/well) were seeded in 96-well plates in RPMI-1640
497 medium supplemented with 10% FCS. After 24 hours, serial dilutions of the tested drugs were
498 added and each concentration was tested in triplicate. After 96 hours, cells were fixed with
499 10% trichloroacetic acid and stained with 0.4% SRB in 1% acetic acid. SRB-fixed cells were
500 dissolved in 10 mmol/L Tris–HCl and absorbance at 540 nm was read using an MRX plate
501 reader (Dynex, Inc., Vienna, VA, USA). IC50 was determined graphically from the
502 cytotoxicity curves.
503 For HCT116-*shYAP/siTAZ*, cells were transfected in 6 well plates 24h before starting the cell
504 growth and cytotoxicity assays.
505
506 ***Quantification of the interaction effect***
507 The interaction between the drugs tested *in vitro* was investigated with a concentration matrix
508 test, in which increasing concentration of each single drug were assessed with all possible
509 combinations of the other drugs. For each combination, the percentage of expected growing
510 cells in the case of effect independence was calculated according to the Bliss equation (Greco
511 et al., 1995):
512 $$fu_c = fu_A fu_B$$
513 where fu_c is the expected fraction of cells unaffected by the drug combination in the case of
514 effect independence, and fu_A and fu_B are the fractions of cells unaffected by treatment *A* and *B,*
515 respectively. The difference between the fu_c value and the fraction of living cells in the
516 cytotoxicity test was considered as an estimation of the interaction effect, with positive values
517 indicating synergism and negative values antagonism.
518
519

520 **REFERENCES**

521 Abuetabh Y, Wu HH, Chai C, Al Yousef H, Persad S, Sergi CM, Leng R. 2022. DNA damage response
522 revisited: the p53 family and its regulators provide endless cancer therapy opportunities.
523 *Exp Mol Med* **54**:1658–1669. doi:10.1038/s12276-022-00863-4
524 Anders S, Huber W. 2010. Differential expression analysis for sequence count data. *Genome Biol*
525 **11**:R106. doi:10.1186/gb-2010-11-10-r106
526 Azzolin L, Panciera T, Soligo S, Enzo E, Bicciato S, Dupont S, Bresolin S, Frasson C, Basso G, Guzzardo
527 V, Fassina A, Cordenonsi M, Piccolo S. 2014. YAP/TAZ incorporation in the β-catenin
528 destruction complex orchestrates the Wnt response. *Cell* **158**:157–170.
529 doi:10.1016/j.cell.2014.06.013
530 Azzolin L, Zanconato F, Bresolin S, Forcato M, Basso G, Bicciato S, Cordenonsi M, Piccolo S. 2012.
531 Role of TAZ as mediator of Wnt signaling. *Cell* **151**:1443–1456.
532 doi:10.1016/j.cell.2012.11.027
533 Barry ER, Morikawa T, Butler BL, Shrestha K, de la Rosa R, Yan KS, Fuchs CS, Magness ST, Smits R,
534 Ogino S, Kuo CJ, Camargo FD. 2013. Restriction of intestinal stem cell expansion and the
535 regenerative response by YAP. *Nature* **493**:106–110. doi:10.1038/nature11693
536 Basu S, Totty NF, Irwin MS, Sudol M, Downward J. 2003. Akt phosphorylates the Yes-associated
537 protein, YAP, to induce interaction with 14-3-3 and attenuation of p73-mediated apoptosis.
538 *Mol Cell* **11**:11–23. doi:10.1016/s1097-2765(02)00776-1
539 Byun MR, Hwang J-H, Kim AR, Kim KM, Park JI, Oh HT, Hwang ES, Hong J-H. 2017. SRC activates TAZ
540 for intestinal tumorigenesis and regeneration. *Cancer Lett* **410**:32–40.
541 doi:10.1016/j.canlet.2017.09.003
542 Chaney S. 1995. The chemistry and biology of platinum complexes with the 1,2-diaminocyclohexane
543 carrier ligand (review). *Int J Oncol* **6**:1291–1305. doi:10.3892/ijo.6.6.1291
544 Cheung P, Xiol J, Dill MT, Yuan W-C, Panero R, Roper J, Osorio FG, Maglic D, Li Q, Gurung B, Calogero
545 RA, Yilmaz ÖH, Mao J, Camargo FD. 2020. Regenerative Reprogramming of the Intestinal
546 Stem Cell State via Hippo Signaling Suppresses Metastatic Colorectal Cancer. *Cell Stem Cell*
547 **27**:590-604.e9. doi:10.1016/j.stem.2020.07.003
548 Di Cara F, Maile TM, Parsons BD, Magico A, Basu S, Tapon N, King-Jones K. 2015. The Hippo pathway
549 promotes cell survival in response to chemical stress. *Cell Death Differ* **22**:1526–1539.
550 doi:10.1038/cdd.2015.10
551 Ege N, Dowbaj AM, Jiang M, Howell M, Hooper S, Foster C, Jenkins RP, Sahai E. 2018. Quantitative
552 Analysis Reveals that Actin and Src-Family Kinases Regulate Nuclear YAP1 and Its Export. *Cell*
553 *Syst* **6**:692-708.e13. doi:10.1016/j.cels.2018.05.006
554 Graham MA, Lockwood GF, Greenslade D, Brienza S, Bayssas M, Gamelin E. 2000. Clinical
555 pharmacokinetics of oxaliplatin: a critical review. *Clin Cancer Res* **6**:1205–1218.
556 Greco WR, Bravo G, Parsons JC. 1995. The search for synergy: a critical review from a response
557 surface perspective. *Pharmacol Rev* **47**:331–385.
558 Guégan J-P, Lapouge M, Voisin L, Saba-El-Leil MK, Tanguay P-L, Lévesque K, Brégeon J, Mes-Masson
559 A-M, Lamarre D, Haibe-Kains B, Trinh VQ, Soucy G, Bilodeau M, Meloche S. 2022. Signaling
560 by the tyrosine kinase Yes promotes liver cancer development. *Sci Signal* **15**:eabj4743.
561 doi:10.1126/scisignal.abj4743
562 Heng BC, Zhang X, Aubel D, Bai Y, Li X, Wei Y, Fussenegger M, Deng X. 2021. An overview of signaling
563 pathways regulating YAP/TAZ activity. *Cell Mol Life Sci* **78**:497–512. doi:10.1007/s00018-020-
564 03579-8
565 Ho KC, Zhou Z, She Y-M, Chun A, Cyr TD, Yang X. 2011. Itch E3 ubiquitin ligase regulates large tumor
566 suppressor 1 stability [corrected]. *Proc Natl Acad Sci U S A* **108**:4870–4875.
567 doi:10.1073/pnas.1101273108
568 Kanai F, Marignani PA, Sarbassova D, Yagi R, Hall RA, Donowitz M, Hisaminato A, Fujiwara T, Ito Y,
569 Cantley LC, Yaffe MB. 2000. TAZ: a novel transcriptional co-activator regulated by

570 interactions with 14-3-3 and PDZ domain proteins. *EMBO J* **19**:6778–6791.
571 doi:10.1093/emboj/19.24.6778
572 Kantar D, Mur EB, Mancini M, Slaninova V, Salah YB, Costa L, Forest E, Lassus P, Géminard C,
573 Boissière-Michot F, Orsetti B, Theillet C, Colinge J, Benistant C, Maraver A, Heron-Milhavet L,
574 Djiane A. 2021. MAGI1 inhibits the AMOTL2/p38 stress pathway and prevents luminal breast
575 tumorigenesis. *Sci Rep* **11**:5752. doi:10.1038/s41598-021-85056-1
576 Kedan A, Verma N, Saroha A, Shreberk-Shaked M, Müller A-K, Nair NU, Lev S. 2018. PYK2 negatively
577 regulates the Hippo pathway in TNBC by stabilizing TAZ protein. *Cell Death Dis* **9**:985.
578 doi:10.1038/s41419-018-1005-z
579 Kim MH, Kim J. 2017. Role of YAP/TAZ transcriptional regulators in resistance to anti-cancer
580 therapies. *Cell Mol Life Sci* **74**:1457–1474. doi:10.1007/s00018-016-2412-x
581 Konsavage WM, Kyler SL, Rennoll SA, Jin G, Yochum GS. 2012. Wnt/β-catenin signaling regulates Yes-
582 associated protein (YAP) gene expression in colorectal carcinoma cells. *J Biol Chem*
583 **287**:11730–11739. doi:10.1074/jbc.M111.327767
584 Kopetz S, Lesslie DP, Dallas NA, Park SI, Johnson M, Parikh NU, Kim MP, Abbruzzese JL, Ellis LM,
585 Chandra J, Gallick GE. 2009. Synergistic activity of the SRC family kinase inhibitor dasatinib
586 and oxaliplatin in colon carcinoma cells is mediated by oxidative stress. *Cancer Res* **69**:3842–
587 3849. doi:10.1158/0008-5472.CAN-08-2246
588 Lamar JM, Xiao Y, Norton E, Jiang Z-G, Gerhard GM, Kooner S, Warren JSA, Hynes RO. 2019. SRC
589 tyrosine kinase activates the YAP/TAZ axis and thereby drives tumor growth and metastasis.
590 *J Biol Chem* **294**:2302–2317. doi:10.1074/jbc.RA118.004364
591 Lapi E, Di Agostino S, Donzelli S, Gal H, Domany E, Rechavi G, Pandolfi PP, Givol D, Strano S, Lu X,
592 Blandino G. 2008. PML, YAP, and p73 are components of a proapoptotic autoregulatory
593 feedback loop. *Mol Cell* **32**:803–814. doi:10.1016/j.molcel.2008.11.019
594 Lee K-W, Lee SS, Kim S-B, Sohn BH, Lee H-S, Jang H-J, Park Y-Y, Kopetz S, Kim SS, Oh SC, Lee J-S. 2015.
595 Significant association of oncogene YAP1 with poor prognosis and cetuximab resistance in
596 colorectal cancer patients. *Clin Cancer Res* **21**:357–364. doi:10.1158/1078-0432.CCR-14-
597 1374
598 Levy D, Adamovich Y, Reuven N, Shaul Y. 2007. The Yes-associated protein 1 stabilizes p73 by
599 preventing Itch-mediated ubiquitination of p73. *Cell Death Differ* **14**:743–751.
600 doi:10.1038/sj.cdd.4402063
601 Li F-L, Guan K-L. 2022. The two sides of Hippo pathway in cancer. *Semin Cancer Biol* **85**:33–42.
602 doi:10.1016/j.semcancer.2021.07.006
603 Li P, Silvis MR, Honaker Y, Lien W-H, Arron ST, Vasioukhin V. 2016. αE-catenin inhibits a Src-YAP1
604 oncogenic module that couples tyrosine kinases and the effector of Hippo signaling
605 pathway. *Genes Dev* **30**:798–811. doi:10.1101/gad.274951.115
606 Li Q, Sun Y, Jarugumilli GK, Liu S, Dang K, Cotton JL, Xiol J, Chan PY, DeRan M, Ma L, Li R, Zhu LJ, Li JH,
607 Leiter AB, Ip YT, Camargo FD, Luo X, Johnson RL, Wu X, Mao J. 2020. Lats1/2 Sustain
608 Intestinal Stem Cells and Wnt Activation through TEAD-Dependent and Independent
609 Transcription. *Cell Stem Cell* **26**:675-692.e8. doi:10.1016/j.stem.2020.03.002
610 Lignitto L, Arcella A, Sepe M, Rinaldi L, Delle Donne R, Gallo A, Stefan E, Bachmann VA, Oliva MA,
611 Tiziana Storlazzi C, L'Abbate A, Brunetti A, Gargiulo S, Gramanzini M, Insabato L, Garbi C,
612 Gottesman ME, Feliciello A. 2013. Proteolysis of MOB1 by the ubiquitin ligase praja2
613 attenuates Hippo signalling and supports glioblastoma growth. *Nat Commun* **4**:1822.
614 doi:10.1038/ncomms2791
615 Ling H-H, Kuo C-C, Lin B-X, Huang Y-H, Lin C-W. 2017. Elevation of YAP promotes the epithelial-
616 mesenchymal transition and tumor aggressiveness in colorectal cancer. *Exp Cell Res*
617 **350**:218–225. doi:10.1016/j.yexcr.2016.11.024
618 Liu-Chittenden Y, Huang B, Shim JS, Chen Q, Lee S-J, Anders RA, Liu JO, Pan D. 2012. Genetic and
619 pharmacological disruption of the TEAD-YAP complex suppresses the oncogenic activity of
620 YAP. *Genes Dev* **26**:1300–1305. doi:10.1101/gad.192856.112

621 Miyajima C, Kawarada Y, Inoue Y, Suzuki C, Mitamura K, Morishita D, Ohoka N, Imamura T, Hayashi
622 H. 2020. Transcriptional Coactivator TAZ Negatively Regulates Tumor Suppressor p53
623 Activity and Cellular Senescence. *Cells* **9**:171. doi:10.3390/cells9010171
624 Morice S, Mullard M, Brion R, Dupuy M, Renault S, Tesfaye R, Brounais-Le Royer B, Ory B, Redini F,
625 Verrecchia F. 2020. The YAP/TEAD Axis as a New Therapeutic Target in Osteosarcoma: Effect
626 of Verteporfin and CA3 on Primary Tumor Growth. *Cancers (Basel)* **12**:3847.
627 doi:10.3390/cancers12123847
628 Nguyen CDK, Yi C. 2019. YAP/TAZ Signaling and Resistance to Cancer Therapy. *Trends Cancer* **5**:283–
629 296. doi:10.1016/j.trecan.2019.02.010
630 Panatta E, Zampieri C, Melino G, Amelio I. 2021. Understanding p53 tumour suppressor network.
631 *Biol Direct* **16**:14. doi:10.1186/s13062-021-00298-3
632 Perego P, Robert J. 2016. Oxaliplatin in the era of personalized medicine: from mechanistic studies
633 to clinical efficacy. *Cancer Chemother Pharmacol* **77**:5–18. doi:10.1007/s00280-015-2901-x
634 Pocaterra A, Romani P, Dupont S. 2020. YAP/TAZ functions and their regulation at a glance. *J Cell Sci*
635 **133**:jcs230425. doi:10.1242/jcs.230425
636 Raudvere U, Kolberg L, Kuzmin I, Arak T, Adler P, Peterson H, Vilo J. 2019. g:Profiler: a web server for
637 functional enrichment analysis and conversions of gene lists (2019 update). *Nucleic Acids Res*
638 **47**:W191–W198. doi:10.1093/nar/gkz369
639 Rawla P, Sunkara T, Barsouk A. 2019. Epidemiology of colorectal cancer: incidence, mortality,
640 survival, and risk factors. *Prz Gastroenterol* **14**:89–103. doi:10.5114/pg.2018.81072
641 Raymond E, Faivre S, Woynarowski JM, Chaney SG. 1998. Oxaliplatin: mechanism of action and
642 antineoplastic activity. *Semin Oncol* **25**:4–12.
643 Reggiani F, Gobbi G, Ciarrocchi A, Sancisi V. 2021. YAP and TAZ Are Not Identical Twins. *Trends*
644 *Biochem Sci* **46**:154–168. doi:10.1016/j.tibs.2020.08.012
645 Rosenbluh J, Nijhawan D, Cox AG, Li X, Neal JT, Schafer EJ, Zack TI, Wang X, Tsherniak A, Schinzel AC,
646 Shao DD, Schumacher SE, Weir BA, Vazquez F, Cowley GS, Root DE, Mesirov JP, Beroukhim R,
647 Kuo CJ, Goessling W, Hahn WC. 2012. β-Catenin-driven cancers require a YAP1
648 transcriptional complex for survival and tumorigenesis. *Cell* **151**:1457–1473.
649 doi:10.1016/j.cell.2012.11.026
650 Salah Z, Melino G, Aqeilan RI. 2011. Negative regulation of the Hippo pathway by E3 ubiquitin ligase
651 ITCH is sufficient to promote tumorigenicity. *Cancer Res* **71**:2010–2020. doi:10.1158/0008-
652 5472.CAN-10-3516
653 Shao DD, Xue W, Krall EB, Bhutkar A, Piccioni F, Wang X, Schinzel AC, Sood S, Rosenbluh J, Kim JW,
654 Zwang Y, Roberts TM, Root DE, Jacks T, Hahn WC. 2014. KRAS and YAP1 converge to regulate
655 EMT and tumor survival. *Cell* **158**:171–184. doi:10.1016/j.cell.2014.06.004
656 Sirvent A, Mevizou R, Naim D, Lafitte M, Roche S. 2020. Src Family Tyrosine Kinases in Intestinal
657 Homeostasis, Regeneration and Tumorigenesis. *Cancers (Basel)* **12**:E2014.
658 doi:10.3390/cancers12082014
659 Song S, Xie M, Scott AW, Jin J, Ma L, Dong X, Skinner HD, Johnson RL, Ding S, Ajani JA. 2018. A Novel
660 YAP1 Inhibitor Targets CSC-Enriched Radiation-Resistant Cells and Exerts Strong Antitumor
661 Activity in Esophageal Adenocarcinoma. *Mol Cancer Ther* **17**:443–454. doi:10.1158/1535-
662 7163.MCT-17-0560
663 Steinhardt AA, Gayyed MF, Klein AP, Dong J, Maitra A, Pan D, Montgomery EA, Anders RA. 2008.
664 Expression of Yes-associated protein in common solid tumors. *Hum Pathol* **39**:1582–1589.
665 doi:10.1016/j.humpath.2008.04.012
666 Strano S, Monti O, Pediconi N, Baccarini A, Fontemaggi G, Lapi E, Mantovani F, Damalas A, Citro G,
667 Sacchi A, Del Sal G, Levrero M, Blandino G. 2005. The transcriptional coactivator Yes-
668 associated protein drives p73 gene-target specificity in response to DNA Damage. *Mol Cell*
669 **18**:447–459. doi:10.1016/j.molcel.2005.04.008

670 Strano S, Munarriz E, Rossi M, Castagnoli L, Shaul Y, Sacchi A, Oren M, Sudol M, Cesareni G, Blandino
671 G. 2001. Physical interaction with Yes-associated protein enhances p73 transcriptional
672 activity. *J Biol Chem* **276**:15164–15173. doi:10.1074/jbc.M010484200
673 Tapon N, Harvey KF, Bell DW, Wahrer DCR, Schiripo TA, Haber DA, Hariharan IK. 2002. salvador
674 Promotes both cell cycle exit and apoptosis in Drosophila and is mutated in human cancer
675 cell lines. *Cell* **110**:467–478. doi:10.1016/s0092-8674(02)00824-3
676 Tesniere A, Schlemmer F, Boige V, Kepp O, Martins I, Ghiringhelli F, Aymeric L, Michaud M, Apetoh L,
677 Barault L, Mendiboure J, Pignon J-P, Jooste V, van Endert P, Ducreux M, Zitvogel L, Piard F,
678 Kroemer G. 2010. Immunogenic death of colon cancer cells treated with oxaliplatin.
679 *Oncogene* **29**:482–491. doi:10.1038/onc.2009.356
680 Thompson BJ. 2020. YAP/TAZ: Drivers of Tumor Growth, Metastasis, and Resistance to Therapy.
681 *Bioessays* **42**:e1900162. doi:10.1002/bies.201900162
682 Totaro A, Panciera T, Piccolo S. 2018. YAP/TAZ upstream signals and downstream responses. *Nat Cell*
683 *Biol* **20**:888–899. doi:10.1038/s41556-018-0142-z
684 Touil Y, Igoudjil W, Corvaisier M, Dessein A-F, Vandomme J, Monté D, Stechly L, Skrypek N, Langlois
685 C, Grard G, Millet G, Leteurtre E, Dumont P, Truant S, Pruvot F-R, Hebbar M, Fan F, Ellis LM,
686 Formstecher P, Van Seuningen I, Gespach C, Polakowska R, Huet G. 2014. Colon cancer cells
687 escape 5FU chemotherapy-induced cell death by entering stemness and quiescence
688 associated with the c-Yes/YAP axis. *Clin Cancer Res* **20**:837–846. doi:10.1158/1078-
689 0432.CCR-13-1854
690 Vasan N, Baselga J, Hyman DM. 2019. A view on drug resistance in cancer. *Nature* **575**:299–309.
691 doi:10.1038/s41586-019-1730-1
692 Wang C, Zhu X, Feng W, Yu Y, Jeong K, Guo W, Lu Y, Mills GB. 2016. Verteporfin inhibits YAP function
693 through up-regulating 14-3-3σ sequestering YAP in the cytoplasm. *Am J Cancer Res* **6**:27–37.
694 Woynarowski JM, Chapman WG, Napier C, Herzig MC, Juniewicz P. 1998. Sequence- and region-
695 specificity of oxaliplatin adducts in naked and cellular DNA. *Mol Pharmacol* **54**:770–777.
696 doi:10.1124/mol.54.5.770
697 Woynarowski JM, Faivre S, Herzig MC, Arnett B, Chapman WG, Trevino AV, Raymond E, Chaney SG,
698 Vaisman A, Varchenko M, Juniewicz PE. 2000. Oxaliplatin-induced damage of cellular DNA.
699 *Mol Pharmacol* **58**:920–927. doi:10.1124/mol.58.5.920
700 Xie Y-H, Chen Y-X, Fang J-Y. 2020. Comprehensive review of targeted therapy for colorectal cancer.
701 *Signal Transduct Target Ther* **5**:22. doi:10.1038/s41392-020-0116-z
702 Yoshikawa K, Noguchi K, Nakano Y, Yamamura M, Takaoka K, Hashimoto-Tamaoki T, Kishimoto H.
703 2015. The Hippo pathway transcriptional co-activator, YAP, confers resistance to cisplatin in
704 human oral squamous cell carcinoma. *Int J Oncol* **46**:2364–2370. doi:10.3892/ijo.2015.2948
705 Zeng R, Dong J. 2021. The Hippo Signaling Pathway in Drug Resistance in Cancer. *Cancers (Basel)*
706 **13**:318. doi:10.3390/cancers13020318
707 Zheng Y, Pan D. 2019. The Hippo Signaling Pathway in Development and Disease. *Dev Cell* **50**:264–
708 282. doi:10.1016/j.devcel.2019.06.003
709

710

711

ACKNOWLEDGEMENTS

The authors thank the different lab members of the Djiane and Gongora teams for helpful discussions. VS was supported by Fondation de France. MR was supported by LabEx NUMEV. DK was supported by Ligue Contre le Cancer. This work was supported by grants from Fondation ARC (#PJA 20141201630) and Ligue Nationale Contre le Cancer (Région Languedoc-Roussillon) to LHM and AD. Work in the lab of CG was also supported by grants and funds from INSERM, the Institut du cancer de Montpellier (ICM), SIRIC (SIRIC Montpellier Cancer Grant «INCa-DGOS-Inserm 6045»), Cancéropole GSO, and the program «investissement d'avenir» (grant agreement: Labex MabImprove, ANR-10-LABX-53-01).

AUTHOR CONTRIBUTIONS

VS, LHM, LJ, and DK performed experiments. CG and AD designed the experiments. VS, LHM, MR, DK, CG and AD analyzed the data. VS, LHM, DT, LB, CG, and AD interpreted the data. CG and AD wrote the manuscript.

COMPETING INTERESTS

All authors declare no competing interest

732 **FIGURE LEGENDS**

733 **Figure 1. Oxaliplatin treatment induces DNA damage**

734 **A**. Immunofluorescence experiments performed on HCT116 cells treated, or not, with
735 oxaliplatin (0.5 μM) monitoring γ-H2AX (yellow). DAPI (blue) was used to stain DNA and
736 the nuclei. Quantification of the staining is shown on the right side and is represented as the
737 corrected nuclear fluorescence. Data are represented as the mean ± SEM. (n=3). Unpaired two-
738 tailed Student's t-test; ** $p<0.01$.

739 **B**. Immunofluorescence experiments performed on HCT116 cells treated, or not, with
740 oxaliplatin (0.5 μM) monitoring 53BP1 (grey). DAPI (blue) was used to stain DNA and the
741 nuclei. Quantification of the staining is shown on the right side and is represented as the
742 corrected nuclear fluorescence. Data are represented as the mean ± SEM. (n=3). Unpaired two-
743 tailed Student's t-test; *** $p<0.001$.

744 **C**. Western blot analysis showing protein expression of TEAD4 and p53 family of proteins in
745 HCT116 treated (Oxa), or not (NT) with oxaliplatin (0.5 μM). GAPDH was used as a loading
746 control (n=3).

747 **D.** Heat map corresponding to the genes differentially expressed in HCT116 cells after 24h of
748 oxaliplatin treatment at IC50 (see Supplemental Table 1). The three replicates for the non-
749 treated (NT) and treated (Oxa) are shown.

750

751 **Figure 2. Oxaliplatin treatment triggers YAP and TAZ nuclear accumulation**

752 **A**. Immunofluorescence experiments performed on HCT116 cells treated, or not, with
753 oxaliplatin (0.5 μM) monitoring TEAD4 (top panels), YAP (middle panels), and TAZ (bottom
754 panels) nuclear localization (red). DAPI (blue) was used to stain DNA and the nuclei.
755 Quantification of both stainings are shown on the right side of the figures and are represented
756 as the corrected nuclear fluorescence. Data are represented as the mean ± SEM (n=3). Unpaired
757 two-tailed Student's t-test; **** $p < 0.0001$.

758 **B**. Western blot analysis showing protein expression and/or activation of Hippo pathway
759 components in HCT116 cells treated (Oxa), or not (NT) with oxaliplatin (0.5 μM). GAPDH
760 was used as a loading control (n=3).

761 **C**. Western blot analysis after subcellular fractionation showing the relative amount of YAP
762 and TAZ protein in the nuclear fraction of HCT116 cells treated (Oxa), or not (NT) with
763 oxaliplatin (0.5 μM). Histone H3 was used as a nuclear loading control for the fractionation
764 (n=3).

765

766 **Figure 3. YAP and TAZ are required for oxaliplatin-mediated cell death**

767 **A**. HCT116-*shYAP* and HCT116-*shLuc* cell lines were treated with increasing doses of
768 oxaliplatin for 96h. Cell viability analysis was then assessed using SRB assay and the IC50 of
769 oxaliplatin was calculated as the concentration needed to kill 50% of the cells (shown in the
770 inset). Paired two-tailed Student's t-test ,* $p<0.05$.

771 **B**. HCT116-*shYAP-siTAZ* and HCT116-*shLuc-siCtl* (control) cell lines were treated with
772 increasing doses of oxaliplatin for 96h. Cell viability analysis was then assessed using SRB
773 assay and the IC50 of oxaliplatin was calculated as the concentration needed to kill 50% of the
774 cells (shown in the inset). Paired two-tailed Student's t-test, ** $p<0.01$.

775 **C**. Western blot analysis showing protein expression of TAZ and YAP in HCT116-*shLuc*, -
776 *siTAZ*, -*shYAP* and both -*shYAP-siTAZ* used in panel A and B. Tubulin was used as a loading
777 control (n=3).

778 **D**. HCT116 cells were incubated with increasing concentrations of oxaliplatin and either
779 Verteporfin or CA3. Cell viability was assessed with the SRB assay in 2D to obtain the viability
780 matrix. Drug concentrations were as follows: Verteporfin (from 0.437 to 7 µM), CA3 (from
781 0.004 to 0.75 µM) and Oxaliplatin (from 0.0185 to 1.2 µM). The synergy matrices were
782 calculated as described in Materials and Methods.

783

784 **Figure 4. Src inhibition by Dasatinib reduces HCT116 cells sensitivity to oxaliplatin**

785 **A**. Western blot analysis showing protein expression of YAP and TAZ in HCT116 treated, or
786 not, with oxaliplatin (0.5 µM) and/or Dasatinib (50 nM and 100 nM). Phopsho-SRC blotting
787 was used to evaluate the inhibition of SRC activity using Dasatinib. GAPDH was used as a
788 loading control (n=3). Quantification of the blots (performed using Image J software) is shown
789 on the right side of the figure.

790 **B**. Immunofluorescence experiments performed in HCT116 cells treated, or not, with
791 oxaliplatin (0.5 µM) and/or Dasatinib (50 nM) monitoring YAP (top panels) and TAZ (bottom
792 panels) nuclear localization (red). DAPI (blue) was used to stain DNA and the nuclei.
793 Quantification of both stainings are shown on the right side of the figures and are represented
794 as the corrected nuclear fluorescence. Data are represented as the mean ± SEM (n=3). Unpaired
795 two-tailed Student's t-test; ****$p < 0.0001$.

796 **C**. HCT116 colorectal cancer cell lines were incubated with increasing concentrations of
797 oxaliplatin and Dasatinib. Cell viability was assessed with the SRB assay in 2D to obtain the
798 viability matrix. Drug concentrations were as follows: Dasatinib (from 1 to 16 µM) and

799 oxaliplatin (from 0.0185 to 1.2 μM). The synergy matrix was calculated as described in
800 Materials and Methods.
801
802
803
804 **SUPPLEMENTAL FIGURE LEGENDS**
805
806 **Supplemental Figure S1. Cell viability in response to drugs**
807 Cells were treated with increasing doses of oxaliplatin (**A**), Verteporfin (**B**), CA3 (**C**) and
808 Dasatinib (**D**) for 96h. Cell viability analysis was then assessed using SRB assay and the IC50
809 of each drug could be calculated as the concentration that reduced cell numbers by 50% (shown
810 in the insets).
811
812 **Supplemental Figure S2. TAZ nuclear accumulation in LoVo and Caco-2 CRC cell lines**
813 **A-B**. Immunofluorescence experiments performed on LoVo (A) and Caco-2 (B) cells treated
814 or not, with oxaliplatin at IC50 (0.6 μM and 0.3 μM respectively) monitoring TAZ nuclear
815 localization (green). DAPI (blue) was used to stain DNA and the nuclei. Quantifications are
816 shown on the right side of the figure and are represented as the corrected nuclear fluorescence.
817 Data are represented as the mean ± SEM. Unpaired two-tailed Student's t-test; **** $p < 0.0001$.
818
819 **Supplemental Figure S3. TAZ mediates sensitivity to oxaliplatin in CRC cell lines**
820 **A**. HCT116-*shYAP-siScramb* (control), HCT116-*shYAP-siTAZ,* and HCT116-*shYAP-siTAZ*
821 transfected with a Flag tagged murine Taz *(pEFmTaz)* cell lines were treated with increasing
822 doses of oxaliplatin for 96h. Cell viability analysis was then assessed using SRB assay and the
823 IC50 of oxaliplatin was calculated as the concentration needed to kill 50% of the cells. Paired
824 two-tailed Student's t-test, ** $p<0.01$, ns non-significant.
825 **B**. Western blot analysis showing protein expression of TAZ and Flag in the different cell lines
826 used in panel A. GAPDH was used as a loading control.
827 **C-D**. LoVo (C) and Caco-2 (D) cells were incubated with increasing concentrations of
828 oxaliplatin and either Verteporfin or CA3. Cell viability was assessed with the SRB assay in
829 2D to obtain the viability matrix. Drug concentrations were as follows: Verteporfin (from 0.875
830 to 14 μM), CA3 (from 0.15 to 2.4 μM) and Oxaliplatin (from 0.075 to 4.8 μM). The synergy
831 matrices were calculated as described in Materials and Methods.
832

833 **Supplemental Figure S4. Interaction between YAP/TAZ and P53 protein family members**
834 **in HCT116 cells**
835 Western blot analysis of Flag (YAP or TAZ) immunoprecipitates on protein extracts from
836 HCT116 treated (Oxa), or not (NT) showing an interaction between YAP and p73 (n=3).
837
838
839 **Supplemental Table 1. Differentially expressed genes in HCT116 cells after oxaliplatin**
840 **treatment for 24h at IC50**
841 Only differentially expressed genes with an adjusted p-value< 0.05 are shown. Columns are:
842 test_id: position and description of the feature tested
843 ENSG_ID: Ensemble gene ID
844 symbol: gene symbol
845 sample_1: first group in the comparison; untreated cells
846 sample_2: second group in the comparison; cells treated with oxaliplatin
847 mean_1: mean of normalized count for the first group in the comparison
848 mean_2: mean of normalized count for the second group in the comparison
849 log2FoldChange: log2 fold change estimates
850 pvalue: pvalue
851 padj: pvalue adjusted for multiple testing with the Benjamini-Hochberg procedure, which
852 controls false discovery rate (FDR)
853
854 **Supplemental Table 2. g:profiler functional enrichment analyses**
855 Columns are :
856 GO_ID: Gene Ontology
857 KEGG_ID: KEGG pathways
858 REAC_ID: Reactome pathways
859 WP_ID: WikiPathways
860 TF_ID: regulatory motif matches from TRANSFAC
861 MIRNA_ID: miRNA targets from miRTarBase
862 CORUM_ID: protein complexes from CORUM
863 HPA_ID: tissue specificity from Human Protein Atlas
864 HP_ID: human disease phenotypes from Human Phenotype Ontology
865
866 Description: description of the functional group

867 p.Val: p-value

868 FDR: false discovery rate

869 Genes: genes found in the intersection

870

871 **Supplemental Table 3. RNA-Seq statistics**

872

Slaninova et al. Figure 1

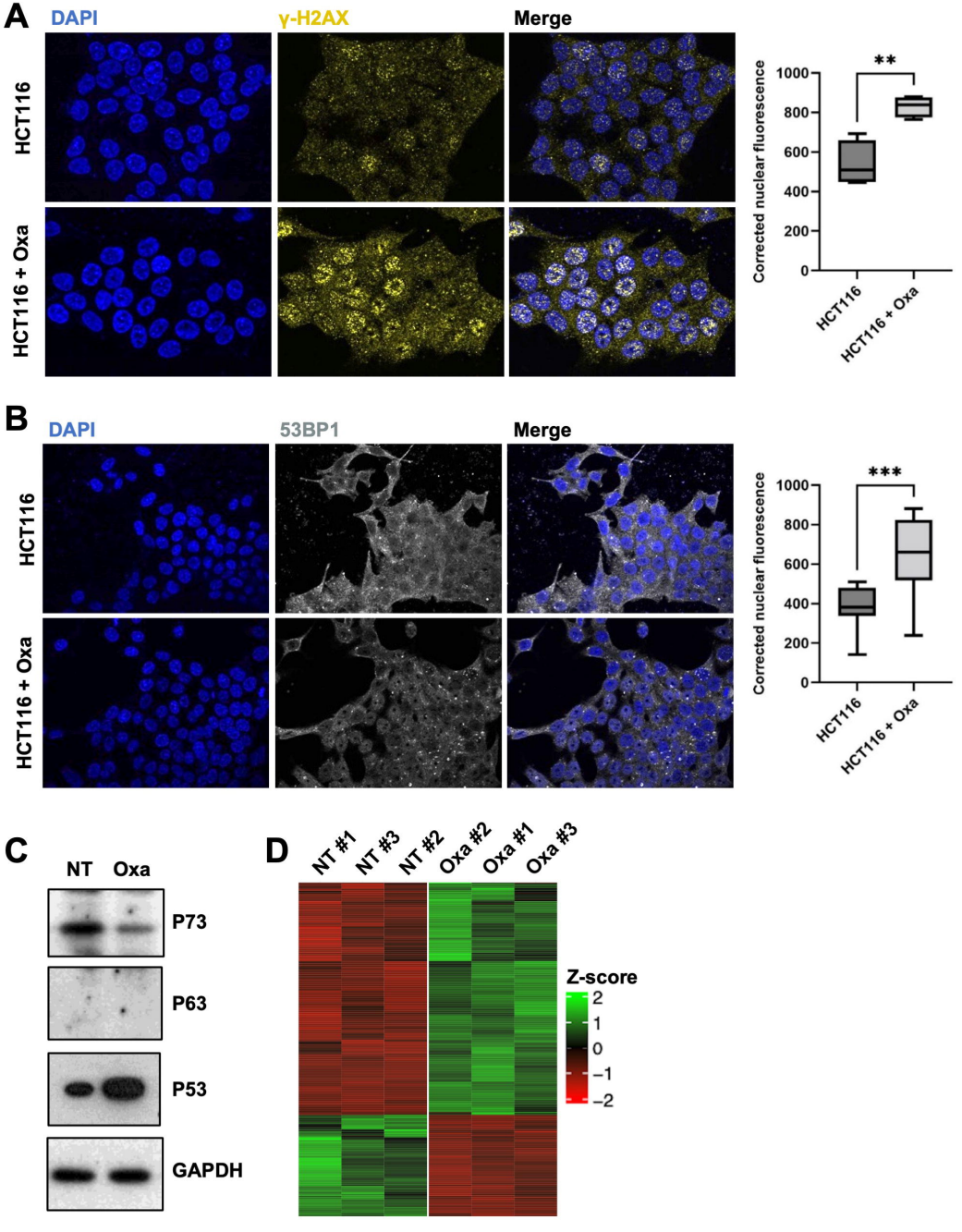

Slaninova et al. Figure 2

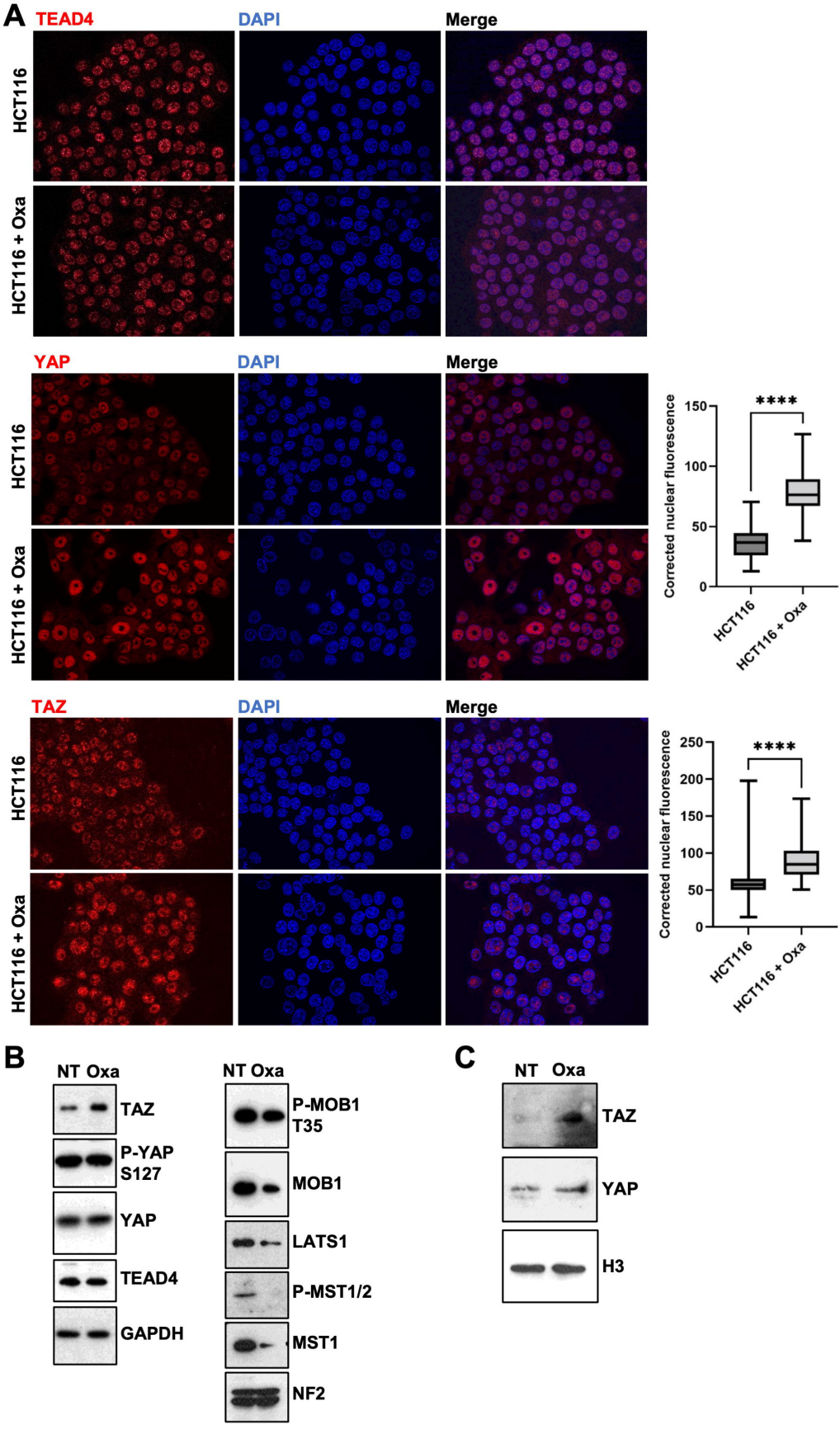

Slaninova et al. Figure 3

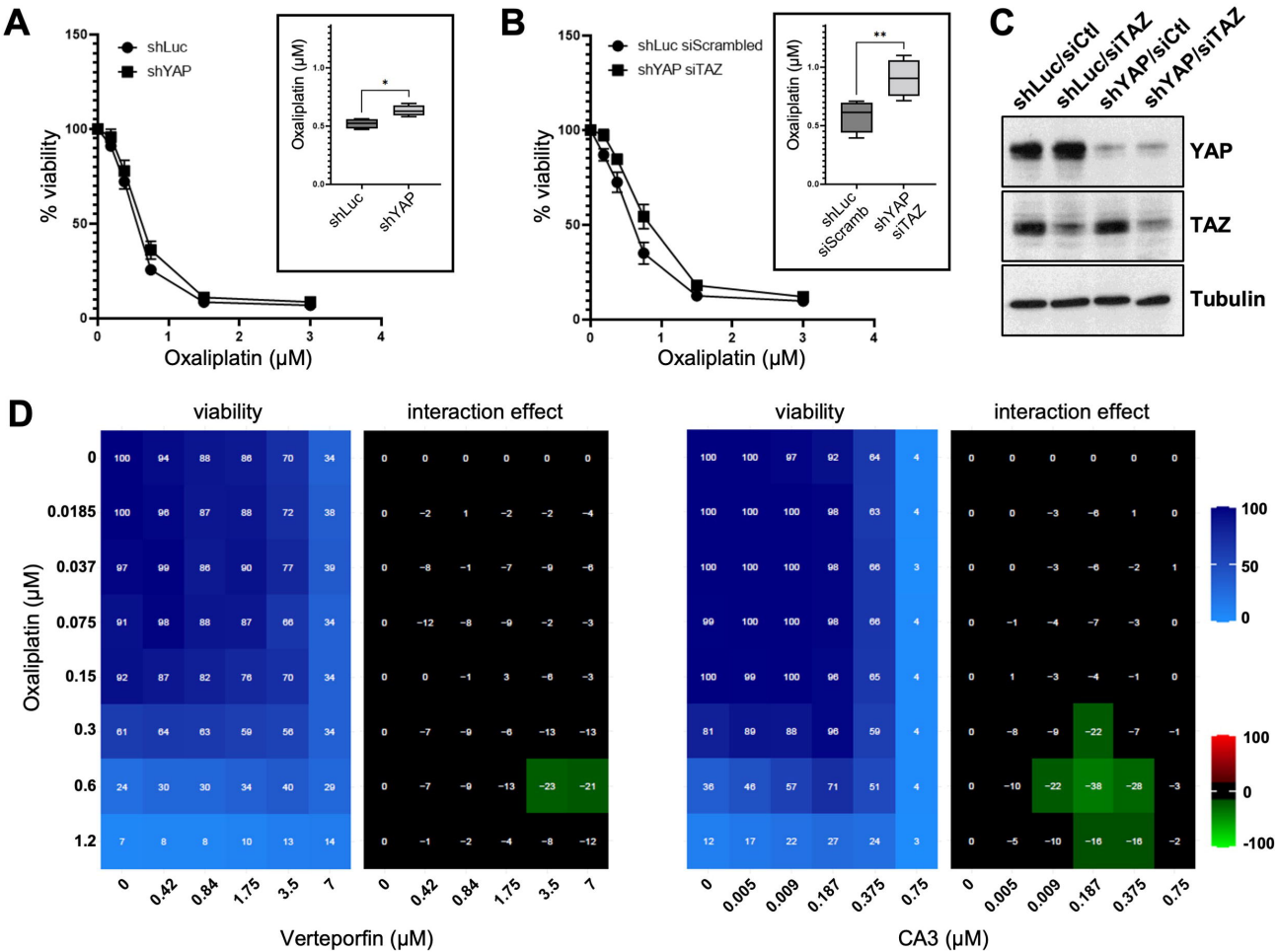

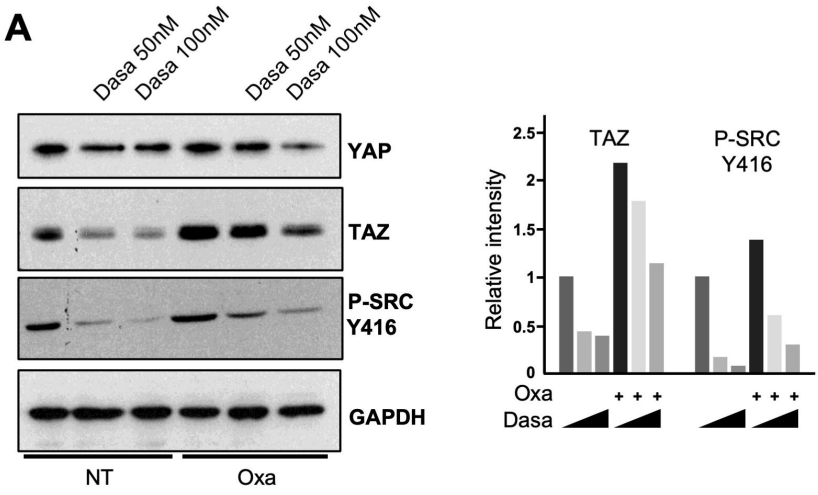
A
Dasa 50nM
Dasa 100nM
Dasa 50nM
Dasa 100nM
YAP
TAZ
P-SRC Y416
GAPDH
NT
Oxa
TAZ
P-SRC Y416
Relative intensity
2.5
2
1.5
1
0.5
0
Oxa
Dasa
+ + +
+ + +

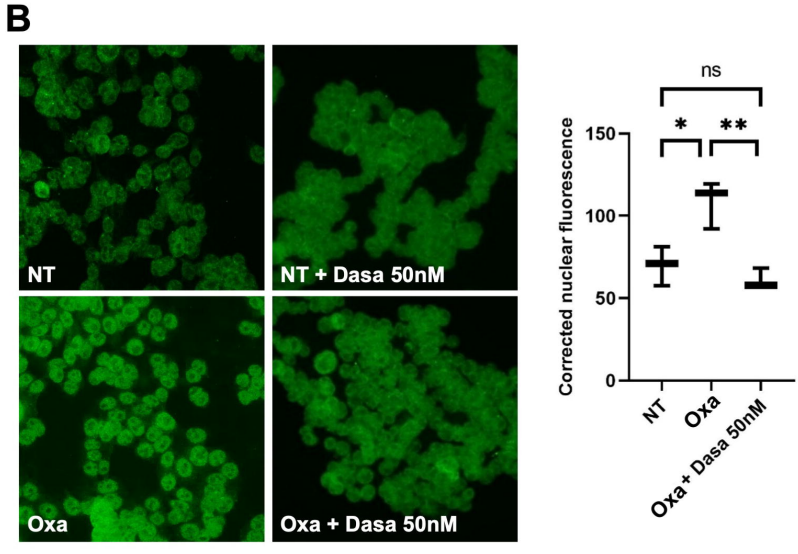
B
NT
NT + Dasa 50nM
Oxa
Oxa + Dasa 50nM
ns
*
**
Corrected nuclear fluorescence
150
100
50
0
NT
Oxa
Oxa + Dasa 50nM

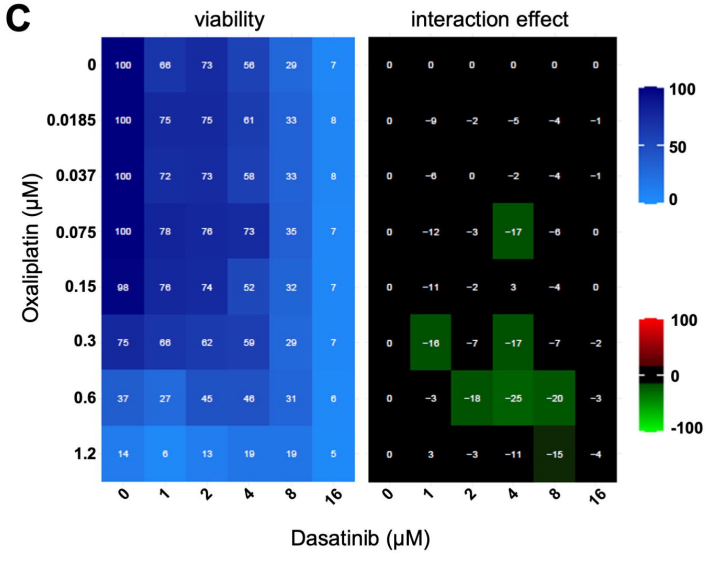
C
viability
interaction effect
Oxaliplatin (μM)
0
0.0185
0.037
0.075
0.15
0.3
0.6
1.2
0 1 2 4 8 16
Dasatinib (μM)
100
50
0
100
0
-100